

THE EFFECT OF FERMI MOMENTUM CUTOFF ON THE BINDING ENERGY OF CLOSED-SHELL NUCLEI IN THE LOCV FRAMEWORK

H. Mariji^a, M. Modarres^{b,1}

^a Department of Physics, K. N. Toosi University of Technology, Tehran

^b Department of Physics, Tehran University, Tehran

The ground-state binding energies of the light symmetric closed-shell nuclei, i.e., ${}^4\text{He}$, ${}^{12}\text{C}$, ${}^{16}\text{O}$ and ${}^{40}\text{Ca}$, and the heavy asymmetric ones, i.e., ${}^{48}\text{Ca}$, ${}^{90}\text{Zr}$ and ${}^{120}\text{Sn}$, are calculated in the harmonic oscillator (HOS) basis, by imposing the relative Fermi momentum cutoff of two point-like interacting nucleons on the density-dependent average effective interactions (DDAEI). The DDAEI are generated through the lowest order constrained variational (LOCV) method calculations for the asymmetric nuclear matter with the operator and the channel-dependent-type bare nucleon–nucleon potentials, such as the Argonne $\text{Av}_{18}^{j_{\text{max}}=2}$ and the Reid soft core, Reid68, interactions. In the framework of the harmonic oscillator shell model, the cutoff is imposed by defining the maximum value of the relative quantum numbers (RQN_{max}) in two ways: (1) the RQN_{max} of the last shell and (2) the RQN_{max} of each shell, in the ground state of the nucleus. It is shown that present results on the binding energies and the root-mean-square radius are closer to the corresponding experimental data than our previous works with the same DDAEI potentials, but without the cutoff constraint. However, for the light symmetric nuclei, the second scheme gives less binding energy and larger root-mean-square radius compared to the first one, while the situation is reversed for the heavier nuclei.

В представленной работе энергии связи основного состояния легких симметричных ядер с замкнутыми оболочками, а именно: ${}^4\text{He}$, ${}^{12}\text{C}$, ${}^{16}\text{O}$ и ${}^{40}\text{Ca}$, и тяжелых асимметричных, ${}^{48}\text{Ca}$, ${}^{90}\text{Zr}$ и ${}^{120}\text{Sn}$, вычисляются в приближении гармонического осциллятора (ГО) с наложением требования относительного импульсного обрезания Ферми двух точечноподобных взаимодействующих ядер на средние эффективные взаимодействия, зависящие от плотности (СЭВЗП). СЭВЗП генерируются вариационным методом наименьшего порядка (ВМНП) для асимметричной ядерной материи и нуклон-нуклонных потенциалов взаимодействия «голых» нуклонов, зависящих от каналов, таких как аргонский $\text{Av}_{18}^{j_{\text{max}}=2}$ и рейдовский с мягким кором Reid68. В рамках оболочечной модели гармонического осциллятора обрезание налагается определением максимального значения относительных квантовых чисел (RQN_{max}) одним из двух способов: 1) RQN_{max} последней оболочки, 2) RQN_{max} каждой оболочки ядра в основном состоянии. Показано, что полученные значения энергии связи и среднеквадратичного радиуса ближе к соответствующим экспериментальным данным, чем наши результаты с теми же СЭВЗП потенциалами, но без обрезания. Однако для легких симметричных ядер вторая схема уменьшает энергию связи и увеличивает среднеквадратичный радиус, если сравнивать ее с первой. В то же время для тяжелых ядер ситуация обратная.

PACS: 21.10.Dr; 21.60.Gx; 27.20.+n; 27.40.+z

¹Corresponding author; e-mail: mmodarres@ut.ac.ir; tel.: +98-21-61118645; fax:+98-21-88004781.

INTRODUCTION

Nowadays, as many decades ago, the main task in the nuclear structure physics is to perform the microscopic many-body calculations to understand the properties, e.g., the binding energies, the root-mean-square radius, etc., of nuclei with A interacting nucleons. It is well known that there is a strong compensation between the nucleon–nucleon (NN) attraction at the intermediate distances $\simeq 1.5$ fm and the significantly stronger repulsion at short distances ≤ 0.5 fm, which leads to the binding energy per nucleon, that is much smaller than both the average kinetic and potential energies [1]. However, the highly complicated nature of NN force and, especially, the presence of a very strong repulsion force at the short distances have made the solution of the nuclear structure problems a difficult task, for the nuclear physics community. To overcome this complication, one of the successful approaches is to use the traditional shell-model approximation with the two-nucleon effective interactions derived from the bare NN potential as its input. However, the two-nucleon effective interaction carries the high-momentum components associated with the strong short-range repulsion, and this momentum is substantially larger than Fermi momentum characteristic of the given nucleus [2,3]. In these regards, by using the lowest order constrained variational (LOCV) method [4–6] and the basic local density Brueckner G-matrix idea [7–9], the density-dependent average effective interaction (DDAEI) as well as the channel- and density-dependent effective interaction (CDDEI) were generated with both the old phenomenological bare NN potentials, i.e., Reid68, Δ –Reid68 and Reid68Day [10,11], and the modern ones, i.e., $Av_{18}^{j_{\max}=2,5}$ [12], and applied to the binding energy calculations of some light, moderate and heavy closed-shell nuclei [13–17]. Although the results were not good in the DDAEI case, in particular for light nuclei, they were good in the CDDEI approaches with respect to our past works as well as others reports [18,19] (see Tables 5, 4 and 8 of references [13,14] and [15], respectively).

Recently, starting from a realistic NN potential and integrating out, in the sense of the *renormalization* group, the high-momentum components of NN , a low-momentum potential, $V_{\text{low-}k}$, was constructed which preserves the physics of the original NN potential up to a certain cutoff momentum Λ [20,21]. To calculate the ground-state properties of some light nuclei in the $V_{\text{low-}k}$ technique, the cutoff momentum is related to the dimension of the configuration space in the coordinate representation [22]. It seems to be a good approximation to consider a cutoff Fermi momentum of the two interacting nucleons through the value of their shell quantum numbers corresponding to the nucleon configurations in each nucleus. In this way, the relative Fermi momenta larger than the cutoff ones are removed from the calculation of DDAEI according to their energy level in the shell model. As will be explained in Sec.1 of this work, this can be done in two schemes: first, according to the maximum value of relative quantum number (RQN) of the two nucleons in the *last shell* in the ground state of the nucleus ($k_c^{\max \text{LS}}$) and, second, in terms of the maximum value of RQN of two nucleons in the *each shell* ($k_c^{\max \text{ES}}$). The harmonic oscillator (HOS) parameter is considered as the varying parameter to calculate the ground-state nucleus binding energy. In Sec.2, the calculated results for symmetric light closed-shell nuclei and asymmetric moderate and heavy ones are presented with DDAEI for both the $Av_{18}^{j_{\max}=2}$ and the Reid68 potentials, which are known as the modern and old phenomenological NN potentials. It is shown that the present results are improved, with respect to our previous calculations [8–12] and regarding the corresponding experimental data.

1. THE BINDING ENERGY WITH THE CUTOFF FERMI MOMENTUM

Similar to our previous works [13–17], the ground-state binding energy of a closed-shell nucleus is calculated in the HOS basis, $|n_i, l_i, j_i, \gamma\rangle$, where n_i , l_i , and j_i are the familiar, principle and orbital and total angular momentum quantum numbers of the nucleons. Again, the HOS parameter $\gamma = \sqrt{M\omega/\hbar}$ is left as a single variational parameter to fix the root-mean-square (rms) radius of the specific nucleus. The nucleon configurations of the closed-shell nuclei, i.e., ${}^4\text{He}$, ${}^{12}\text{C}$, ${}^{16}\text{O}$, ${}^{40}\text{Ca}$, ${}^{48}\text{Ca}$, ${}^{90}\text{Zr}$ and ${}^{120}\text{Sn}$, are chosen similar to our past reports. The calculations are done at the center of mass of the nuclei, and the (average) binding energies per nucleon for the foregoing closed-shell nuclei are written as follows:

$$\frac{\overline{BE}}{A} = (T_1 - T_{\text{cm}}^A) + \overline{E}_2, \quad (1)$$

where

$$T_1 = \sum \left(2n_i + l_i + \frac{3}{2} \right) \frac{\hbar\omega}{2A} \quad (2)$$

is the one-body kinetic energy per nucleon,

$$T_{\text{cm}}^A = \frac{3}{4}\hbar\omega \quad (3)$$

is the energy contribution from the center-of-mass motion and, finally, \overline{E}_2 is the energy contribution from the DDAEI, as follows:

$$\overline{E}_2 = \frac{1}{2} \sum_{ij} \langle ij; \gamma | \overline{V}_{\text{eff}}(1, 2) | ij; \gamma \rangle_a = \overline{T}_{2\text{eff}} + \overline{V}_{2\text{eff}}. \quad (4)$$

The two-body DDAEI operator, $\overline{V}_{\text{eff}}(1, 2)$ [8,10], has the following form:

$$\overline{V}_{\text{eff}}(1, 2) = \frac{-\hbar^2}{2m} [\overline{F}(1, 2), [\nabla_{12}^2, \overline{F}(1, 2)]] + \overline{F}(1, 2)V(12)\overline{F}(1, 2), \quad (5)$$

where $\overline{F}(1, 2)$ and $V(12)$ are the two-body average correlation function [8,10] and the phenomenological NN potential, respectively. As before, the DDAEI, $\overline{V}_{\text{eff}}(1, 2)$, are divided into the two-body effective kinetic and potential portions to consider the behavior of DDAEI in detail (see Eqs.(4) and (5)). In order to speed up our numerical calculations, the local density approximation (LDA) [7–9, 13–17] is assumed. According to Eqs.(24) and (25) of reference [13] or Eqs.(A.33) and (A.34) of reference [15], both the effective state averaged two-body potential and the correlation function depend on the relative distance of the two nucleons and their density. Thus, our DDAEI depends through the well-known relation, to the Fermi momentum, as follows:

$$\rho = \frac{\nu}{6\pi^2} k_F^3, \quad (6)$$

where ν , the spin and the isospin degeneracy of the nucleon, is equal to 4. Now, we are ready to impose the cutoff constraint on the relative Fermi momentum of two nucleons, according to their energy in the corresponding shell model:

$$E_c = \frac{\hbar^2 k_c^2}{M}, \quad (7)$$

and then,

$$k_c = \sqrt{N_c + \frac{3}{2}\gamma}, \quad (8)$$

where k_c and N_c are the cutoff relative Fermi momentum and the cutoff RQN of the corresponding shell. As mentioned before, k_c can be fixed in two ways. First, E_c is limited to the maximum value of the RQN of the last shell in each nucleus, i.e., $k_c^{\max \text{LS}}$. In this case, N_c is defined as

$$N_c^{\max \text{LS}} = 2n_{\max} + l_{\max}, \quad (9)$$

where n_{\max} and l_{\max} are the maximum values of the relative principle and the angular momentum of the nucleons in the last shell of the specific nucleus. Thus, for the ground state of each nucleus, $N_c^{\max \text{LS}}$ can be calculated through its shell model structure, and one finds only one value for $N_c^{\max \text{LS}}$ or $k_c^{\max \text{LS}}$ for each nucleus. However, it should be noted that for the asymmetric nuclei, $N_c^{\max \text{LS}}$ is different for the protons and the neutrons, and we find two values, i.e., $N_{c_p}^{\max \text{LS}}$ and $N_{c_n}^{\max \text{LS}}$ (see Sec. 2 for their corresponding values).

In the second scheme, E_c is limited up to the maximum values of RQN in each shell, i.e., $E_c^{\max \text{ES}}$. In this case in each shell, due to energy conservation, the maximum value of n and l can be derived from the familiar relation: $2n_1 + l_1 + 2n_2 + l_2 = 2n + l + 2N + L$, in which N and L are the center-of-mass principle and angular momentum quantum numbers of the two nucleons, respectively. Thus, $E_c^{\max \text{ES}}$ is calculated in each shell as follows:

$$E_c^{\max \text{ES}} = 2(n_1 + n_2) + l_1 + l_2. \quad (10)$$

So, in this case, we find several $k_c^{\max \text{ES}}$ for each nucleus (see Sec. 2 for their values and the related discussions).

2. RESULTS AND DISCUSSION

Table 1 shows the values of $N_c^{\max \text{LS}}$ for the different closed-shell nuclei, considered in this work. The corresponding $k_c^{\max \text{LS}}$ for each nucleus and the $\text{Av}_{18}^{j_{\max}=2}$ (A) and Reid68 (R) potentials are given in the second column of Table 2. As one expects, the $k_c^{\max \text{LS}}$ are increasing as the atomic mass number is increased. On the other hand, their values are different for each potential, since the calculated

Table 1. The maximum values of RQN of two nucleons in the last shell, $N_c^{\max \text{LS}}$, of some closed-shell symmetric and asymmetric nuclei (see the text for more explanations)

Symmetric				
Nucleus	^4He	^{12}C	^{16}O	^{40}Ca
$N_c^{\max \text{LS}}$	0	2	2	4
Asymmetric				
Nucleus	^{48}Ca	^{90}Zr	^{120}Sn	
$N_{c_p}^{\max \text{LS}}$	4	6	8	
$N_{c_n}^{\max \text{LS}}$	6	8	8	

saturation points are different for the two potentials in each nucleus (see Eq.(8)). The $k_c^{\max \text{LS}}$ values of the asymmetric nuclei are written in the parenthesis for the neutron and the proton configurations, respectively. Obviously, the $k_c^{\max \text{LS}}$ values for neutrons are larger than for protons in the case of asymmetric nuclei. In the third column the values of $k_c^{\max \text{ES}}$ are given for various nuclei, but only for the $\text{Av}_{18}^{j_{\max}=2}$ interaction. Since there is not much difference between the $k_{c_p}^{\max \text{ES}}$ and $k_{c_n}^{\max \text{ES}}$ values, the latter are given. For ^4He there is not any difference between the

Table 2. The Fermi momenta cutoff of the ${}^4\text{He}$, ${}^{12}\text{C}$, ${}^{16}\text{O}$, ${}^{40}\text{Ca}$, ${}^{48}\text{Ca}$, ${}^{90}\text{Zr}$ and ${}^{120}\text{Sn}$ nuclei. Note that the values of $k_c^{\text{max LS}}$ (fm^{-1}) and $k_c^{\text{max ES}}$ (fm^{-1}) are calculated in the saturation points of each nucleus, according to $\text{Av}_{18}^{j_{\text{max}}=2}$ and Reid68 potentials which are assigned «A» and «R», respectively. The values of $k_c^{\text{max ES}}$ are sorted by increasing the amounts of N_c . The $k_c^{\text{max LS}}$ values of asymmetric nuclei are written in parenthesis for neutron and proton configurations. Since there is not much difference between $k_{c_n}^{\text{max ES}}$ and $k_{c_p}^{\text{max ES}}$ in each shell, the values of $k_{c_n}^{\text{max ES}}$ are presented

Nucleus	$k_c^{\text{max LS}}$	$k_c^{\text{max ES}}$
${}^4\text{He}(A)$	0.75	0.75
${}^4\text{He}(R)$	0.72	0.72
${}^{12}\text{C}(A)$	1.03	0.66, 0.85, 1.01
${}^{12}\text{C}(R)$	1.03	0.64, 0.82, 0.97
${}^{16}\text{O}(A)$	1.14	0.70, 0.90, 1.07
${}^{16}\text{O}(R)$	1.12	0.68, 0.88, 1.05
${}^{40}\text{Ca}(A)$	1.36	0.71, 0.92, 1.08, 1.23, 1.36
${}^{40}\text{Ca}(R)$	1.31	0.68, 0.88, 1.05, 1.19, 1.31
${}^{48}\text{Ca}(A)$	(1.424, 1.219)	0.698, 0.901, 1.067, 1.209, 1.337, 1.454, 1.561
${}^{48}\text{Ca}(R)$	(1.452, 1.242)	0.686, 0.886, 1.048, 1.188, 1.314, 1.428, 1.534
${}^{90}\text{Zr}(A)$	(1.573, 1.395)	0.674, 0.870, 1.029, 1.167, 1.290, 1.403, 1.507, 1.604, 1.696
${}^{90}\text{Zr}(R)$	(1.541, 1.368)	0.649, 0.838, 0.992, 1.124, 1.243, 1.351, 1.452, 1.547, 1.634
${}^{120}\text{Sn}(A, R)$	(1.449, 1.448)	0.576, 0.743, 0.879, 0.997, 1.102, 1.198, 1.287, 1.370, 1.449

$k_c^{\text{max LS}}$ and $k_c^{\text{max ES}}$ values, so their numerical values are the same. As the atomic mass increases, the number of shells also increases, and we get more numeric values for $k_c^{\text{max ES}}$. On the other hand, the $k_c^{\text{max ES}}$ values increase as one moves to the higher shells in each nucleus. Note that these cutoff values are calculated at the saturation point of each nucleus (γ) and the values of γ are different in the two schemes, although the potential is the same.

In Fig. 1, the DDAEI of LOCV calculations, with the $\text{Av}_{18}^{j_{\text{max}}=2}$ (Reid68) potential, are plotted for three different values of cutoff Fermi momenta: $k_c^{\text{max LS}} = 0.75$ (0.72), 1.14 (1.12) and 1.34 (1.31) fm^{-1} , corresponding to the maximum values of the RQN of two nucleons in the last shell for the ground state of ${}^4\text{He}$, ${}^{16}\text{O}$ and ${}^{40}\text{Ca}$ nuclei, respectively. The larger variations with respect to $k_c^{\text{max LS}}$ are observed in the case of Reid68. Similarly, in Fig. 2, the same comparisons have been made for one of the asymmetric nuclei for different proton and neutron cutoff Fermi momenta, i.e., ${}^{48}\text{Ca}$, with the magnitudes of $k_{c_p}^{\text{max LS}} = 1.22$ (1.24) fm^{-1} and $k_{c_n}^{\text{max LS}} = 1.42$ (1.45) fm^{-1} , respectively. As in our previous works [14, 16], the data of figures come from the LOCV code for the asymmetric nuclear matter with the asymmetric parameter ($\mathfrak{R} = \rho_p/\rho_n$), which is $\mathfrak{R} = 1.00$ for the symmetric nuclei, in Fig. 1, and $\mathfrak{R} = 0.71$ for the asymmetric nuclei, in Fig. 2, corresponding to the proton-to-neutron ratio of ${}^{48}\text{Ca}$ and ${}^{120}\text{Sn}$ (see also Table 2). The DDAEI are more repulsive for Reid68 potential with respect to the $\text{Av}_{18}^{j_{\text{max}}=2}$ interaction. But the cutoff Fermi momentum values are approximately the same (see Table 2 for their values which correspond to the above figures). On the other hand, according to Fig. 1, the repulsive part of the potential of the two nucleons decreases as the cutoff Fermi momentum is increased for both of the phenomenological interactions. This situation is reversed in the attraction portion of DDAEI potentials. Therefore, it is expected

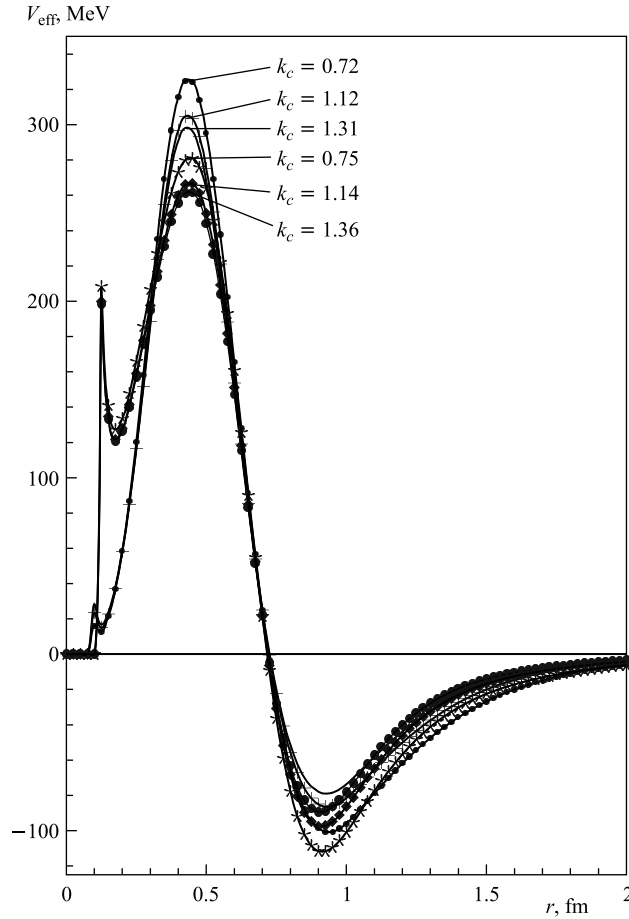


Fig. 1. The DDAEI (MeV) versus the NN relative distance (fm) for the different cutoff Fermi momentum. The heavy solid (solid) curves are for the $Av_{18}^{j_{\max}=2}$ (Reid68). The results are produced by using the asymmetric nuclear matter LOCV code with asymmetric parameters equal to 1

that two nucleons repulse each other in light nuclei much more than in heavier ones. Unlike, the two nucleons are a little more repulsive (attractive) through Reid68 (Av_{18}) interaction than through Av_{18} (Reid68) potential. Although the asymmetric parameter is reduced about thirty percent with respect to the symmetric ones, Fig.2 shows the same situation as Fig. 1 and differences are not very significant. Thus, it seems that the interaction energies of the heavier asymmetric nuclei are not different from those of the symmetric ones with respect to the DDAEI graphs.

The variational binding energies per nucleon (MeV) of the symmetric closed-shell nuclei by using the DDAEI with the $Av_{18}^{j_{\max}=2}$ and the Reid68 potentials are given in Table 3. The first column shows the different nuclei in which the letters « A » and « R » stand for the $Av_{18}^{j_{\max}=2}$ and the Reid68 potentials, respectively. The next two columns show the values of the saturation oscillator parameter γ (fm^{-1}) and the calculated saturation rms radius (fm). The forth up to seventh columns stand for the differences between the single particle and

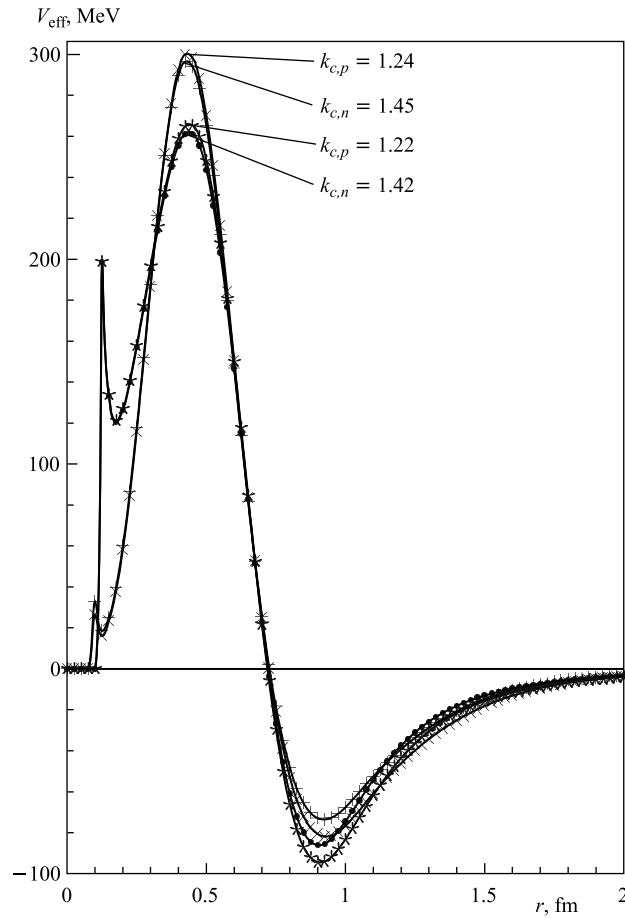


Fig. 2. The same as Fig.1, but with different proton and neutron cutoff Fermi momenta and the asymmetric parameters equal to 0.71

the center-of-mass kinetic energies, the two-body effective kinetic and two-body effective potential energies and the saturation binding energies (MeV). The columns labeled by stars present the binding energy and rms radius of the symmetric nuclei from our previous works, references [15] and [13], respectively, without the inclusion of the cutoff. Finally, the last two columns show the experimental binding energy (MeV) and the rms radius (fm). This table demonstrates that the momentum cutoff increases (decreases) the binding energies (rms) of light closed-shell symmetric nuclei by about 2 MeV (10%) with respect to the same calculation but without the cutoff constraint (the star numbers). Especially, we get very good agreement with the experimental data for the ^{40}Ca nucleus. In the present calculation, while the addition of the one- (especially because of the reduction of the rms radius) and two-body kinetic energies increases by about 20%, there is more than 35% increase in the two-body potential energy (e.g., see Table 1 of reference [15]). So, as one would expect, on average the cutoff constraint forces the nucleons to attract each other more than in the unconstrained case.

Table 3. The variational binding energies (MeV) from the first consideration for the symmetric closed-shell nuclei by using the DDAEI with $Av_{18}(j_{\max} = 2)$ (specified by «A») and Reid68 (specified by «R»). Data characterized by * comes from [15] and [13] corresponding to the $Av_{18}^{j_{\max}=2}$ and Reid68 potentials, respectively. See the text for explanation for different columns

Nucleus	γ	r_{rms}	$\frac{T_1 - T_{\text{cm}}^A}{A}$	$\frac{\bar{T}_2^{\text{eff}}}{A}$	$\frac{\bar{V}_2^{\text{eff}}}{A}$	$\frac{\overline{BE}}{A}$	$\frac{BE^*}{A}$	r_{rms}^*	$\frac{BE^{\text{exp}}}{A}$	r^{exp}
${}^4\text{He}(A)$	0.61	2.01	8.68	6.02	-17.30	-2.60	-0.71	2.66	-7.08	1.63
${}^4\text{He}(R)$	0.59	2.08	8.12	6.76	-17.30	-2.42	-0.79	2.66		
${}^{12}\text{C}(A)$	0.55	3.15	12.80	7.35	-22.34	-2.19	-1.03	2.94	-7.68	2.47
${}^{12}\text{C}(R)$	0.55	3.15	12.80	8.89	-23.79	-2.09	-0.98	2.94		
${}^{16}\text{O}(A)$	0.62	2.42	17.19	12.36	-35.47	-5.92	-2.80	2.73	-7.98	2.65
${}^{16}\text{O}(R)$	0.61	2.46	16.64	14.37	-36.69	-5.69	-2.77	2.83		
${}^{40}\text{Ca}(A)$	0.58	2.99	20.66	15.72	-45.10	-8.71	-5.96	3.21	-8.55	3.39
${}^{40}\text{Ca}(R)$	0.56	3.09	19.26	17.40	-45.06	-8.39	-5.77	3.33		

Table 4. The same as Table 3, but for the asymmetric closed-shell nuclei. The binding energies accounting for the cutoff are characterized by «cut». See the text for more explanation

Nucleus	γ	r_{rms}^n	r_{rms}^p	$\frac{T_1 - T_{\text{cm}}^A}{A}$	$\frac{\bar{T}_2^{\text{eff}}}{A}$	$\frac{\bar{V}_2^{\text{eff}}}{A}$	$\frac{\overline{BE}}{A}$	$\frac{BE^{\text{exp}}}{A}$	r^{exp}
${}^{48}\text{Ca}(A)$	0.54	3.43	3.21	19.46	13.30	-38.34	-5.59	-8.67	3.53
${}^{48}\text{Ca}_{\text{cut}}(A)$	0.52	3.56	3.27	18.04	12.34	-36.71	-6.32		
${}^{48}\text{Ca}(R)$	0.51	3.63	3.40	17.36	13.94	-36.73	-5.44		
${}^{48}\text{Ca}_{\text{cut}}(R)$	0.53	3.49	3.21	18.75	15.52	-40.55	-6.29		
${}^{90}\text{Zr}(A)$	0.52	3.89	3.70	22.02	16.17	-46.43	-8.24	-8.71	4.27
${}^{90}\text{Zr}_{\text{cut}}(A)$	0.51	3.96	3.77	21.18	15.65	-45.78	-8.95		
${}^{90}\text{Zr}(R)$	0.48	4.20	4.02	18.76	16.09	-42.75	-7.89		
${}^{90}\text{Zr}_{\text{cut}}(R)$	0.50	4.04	3.84	20.36	17.93	-47.01	-8.71		
${}^{120}\text{Sn}(A)$	0.47	4.43	4.28	19.79	14.37	-42.97	-8.82	-8.50	4.65
${}^{120}\text{Sn}_{\text{cut}}(A)$	0.47	4.43	4.28	19.79	14.54	-43.87	-9.54		
${}^{120}\text{Sn}(R)$	0.47	4.43	4.28	19.79	17.25	-45.79	-8.74		
${}^{120}\text{Sn}_{\text{cut}}(R)$	0.47	4.43	4.28	19.79	17.46	-46.77	-9.52		

Table 4 is the same as Table 3, but for the asymmetric closed-shell nuclei. The third and the fourth columns show the calculated saturation points of the proton and the neutron rms radius (fm), respectively. Since we have not calculated the binding energies of the asymmetric nuclei with DDAEI in our previous works, these results are presented for both cases, i.e., with (labeled by «cut») and without the cutoff. This table shows that, while for the closed-shell asymmetric nuclei the imposition of the momentum cutoff increases the binding energy of each nucleus by less than an MeV, the rms radius approximately remains the same

Table 5. The same as Table 3 but corresponding to the second consideration. See the text for more explanation

Nucleus	γ	r_{rms}	$\frac{T_1 - T_{\text{cm}}^A}{A}$	$\frac{\overline{T}_2^{\text{eff}}}{A}$	$\frac{\overline{V}_2^{\text{eff}}}{A}$	$\frac{\overline{BE}}{A}$	$\frac{BE^{\text{exp}}}{A}$	r^{exp}
${}^4\text{He}(A)$	0.61	2.01	8.68	6.02	-17.30	-2.60	-7.08	1.63
${}^4\text{He}(R)$	0.59	2.08	8.12	6.76	-17.30	-2.42		
${}^{12}\text{C}(A)$	0.54	3.21	12.34	6.91	-20.96	-1.70	-7.68	2.47
${}^{12}\text{C}(R)$	0.52	3.33	11.45	7.62	-20.67	-1.60		
${}^{16}\text{O}(A)$	0.57	2.63	14.53	9.75	-28.51	-4.24	-7.98	2.65
${}^{16}\text{O}(R)$	0.56	2.68	14.02	11.30	-29.41	-4.10		
${}^{40}\text{Ca}(A)$	0.58	2.99	20.66	15.75	-45.33	-8.91	-8.55	3.39
${}^{40}\text{Ca}(R)$	0.56	3.09	19.26	17.44	-45.28	-8.57		

Table 6. The same as Table 3 but corresponding to the second consideration. See the text for more explanation

Nucleus	γ	r_{rms}^n	r_{rms}^p	$\frac{T_1 - T_{\text{cm}}^A}{A}$	$\frac{\overline{T}_2^{\text{eff}}}{A}$	$\frac{\overline{V}_2^{\text{eff}}}{A}$	$\frac{\overline{BE}}{A}$	$\frac{BE^{\text{exp}}}{A}$	r^{exp}
${}^{48}\text{Ca}(A)$	0.57	3.25	3.04	21.68	15.80	-45.81	-8.33	-8.67	3.53
${}^{48}\text{Ca}(R)$	0.56	3.31	3.09	20.93	18.23	-47.24	-8.08		
${}^{90}\text{Zr}(A)$	0.55	3.68	3.52	24.63	19.46	-56.35	-12.25	-8.71	4.27
${}^{90}\text{Zr}(R)$	0.53	3.81	3.65	22.87	21.45	-56.11	-11.78		
${}^{120}\text{Sn}(A)$	0.47	4.43	4.28	19.79	15.13	-46.93	-12.02	-8.50	4.65
${}^{120}\text{Sn}(R)$	0.47	4.43	4.28	19.79	18.18	-50.09	-12.13		

as in the un-cutoff case and on average the new results are in better agreement with the experimental data.

Tables 5 and 6 are similar to the previous tables, 3 and 4, but by imposing the second scheme, i.e., the $k_c^{\text{max ES}}$ cutoff values from Table 2. The binding energies increase more than in the first scheme and especially for the asymmetric closed-shell nuclei such as ${}^{90}\text{Zr}$ and ${}^{120}\text{Sn}$ and we get up to 3 MeV over binding. On the other hand, the rms radii do not approximately change.

In conclusion, the ground-state binding energies of the light symmetric and the heavy asymmetric closed-shell nuclei, such as ${}^4\text{He}$, ${}^{12}\text{C}$, ${}^{16}\text{O}$, ${}^{40}\text{Ca}$, ${}^{48}\text{Ca}$, ${}^{90}\text{Zr}$ and ${}^{120}\text{Sn}$, were calculated in the harmonic oscillator basis, by imposing the relative Fermi momentum cutoff of the two interacting nucleons on the density-dependent average effective interactions. The density-dependent average effective interactions were generated through the lowest order constrained variational (LOCV) method calculations for the asymmetric nuclear matter with the operator and the channel-dependent type bare nucleon–nucleon potentials, such as the Argonne $\text{Av}_{18}^{j_{\text{max}}=2}$ and the Reid soft core, Reid68, interactions. In the framework of the harmonic oscillator shell model, the cutoff was imposed by defining the maximum value of

the relative quantum numbers in two ways: (i) the maximum value of the relative quantum numbers of the last shell and (ii) the maximum value of the relative quantum numbers of each shell, in the ground state of the nucleus. It was shown that on average the present results on the binding energies, and approximately the root-mean-square radius, are closer to the corresponding experimental data with respect to our previous works with the same DDAEI potentials, but without imposing the cutoff constraint. However, for the light symmetric nuclei, the second scheme gives less binding energy and larger root-means-square radius compared to the first one, while the situation is reversed for the heavier nuclei. As one should expect, it seems that the first scheme is more sensible and suitable, since it is the «last shell» that dictates the «Fermi momentum».

It is expected that one can achieve better results for lighter nuclei, if (1) the truncation on the channel- and density-dependent effective nucleon–nucleon potential is made instead of the average one and (2) all of the interactions Hamiltonian matrix elements [12] are taken into account. On the other hand, one should not ignore the effect of three-body interactions, especially for the light nuclei.

Acknowledgements. H.M. (M.M.) would like to thank the Research Council of K. N. Toosi University of Technology (University of Tehran) for the grants provided for him.

REFERENCES

1. *Bethe H.A.* Theory of Nuclear Matter // *Ann. Rev. Nucl. Part. Sci.* 1971. V. 21. P. 93.
2. *Zabolitsky J.G., Ey W.* Momentum Distributions of Nucleons in Nuclei // *Phys. Lett. B.* 1978. V. 76. P. 527.
3. *Pandharipande V.R., Sick I., deWitt Huberts P.K.A.* Independent Particle Motion and Correlations in Fermion Systems // *Rev. Mod. Phys.* 1997. V. 69. P. 981.
4. *Owen J.C., Bishop R.F., Irvine J.M.* Constrained Variation in Jastrow Method at High Density // *Ann. Phys. (NY)*. 1976. V. 102. P. 170.
5. *Modarres M., Irvine J.M.* LOCV Calculations with a Self-Consistent Treatment of Isobars // *J. Phys. G.* 1979. V. 5. P. 511.
6. *Modarres M., Bordbar G.H.* Incompressibility of Hot Asymmetrical Nuclear Matter: Lowest Order Constrained Variational Approach // *Phys. Rev. C.* 1998. V. 58. P. 2781.
7. *Brueckner K.A., Levinson C.A., Mahmoud H.M.* Two-Body Forces and Nuclear Saturation: I. Central Forces // *Phys. Rev.* 1954. V. 95. P. 217.
8. *Brueckner K.A., Levinson C.A.* Approximate Reduction of the Many-Body Problem for Strongly Interacting Particles to a Problem of Self-Consistent Fields // *Phys. Rev.* 1955. V. 97. P. 1344.
9. *Negele J.W.* Structure of Finite Nuclei in the Local-Density Approximation // *Phys. Rev. C.* 1970. V. 1. P. 1260.
10. *Reid R.V.* Local Phenomenological Nucleon–Nucleon Potentials // *Ann. Phys.* 1968. V. 50. P. 411; *Day B.D.* Three-Body Correlations in Nuclear Matter // *Phys. Rev. C.* 1981. V. 24. P. 1203.
11. *Green A.M., Niskanen J.A., Sainio M.E.* The Effect of the Delta (1236) on the Imaginary Component of Nucleon–Nucleon Phase-Shifts // *J. Phys. G.* 1978. V. 4. P. 1055.
12. *Wiringa R.B., Stocks V.G.J., Schiavilla R.* Accurate Nucleon–Nucleon Potential with Charge-Independence Breaking // *Phys. Rev. C.* 1955. V. 51. P. 38.
13. *Modarres M., Rasekhinejad N.* The Effective Potential and Local Density Approximation Approach to the Binding Energy of Closed Shell Nuclei // *Phys. Rev. C.* 2005 V. 72. P. 014301.

14. *Modarres M., Rasekhinejad N.* Ground State of Heavy Closed Shell Nuclei: An Effective Interaction and Local Density Approximation Approach // *Ibid.* V. 72. P. 064306.
15. *Modarres M., Rasekhinejad N., Mariji H.* The Density-Dependent AV18 Effective Interaction and Ground State of Closed Shell Nuclei // *Intern. J. Mod. Phys. E.* 2011. V. 20, No. 3. P. 679.
16. *Modarres M., Mariji H., Rasekhinejad N.* The Effect of Density-Dependent AV18 Effective Interaction on the Ground State Properties of Heavy Closed Shell Nuclei // *Nucl. Phys. A.* 2011. V. 859. P. 16.
17. *Modarres M., Mariji H.* The Effect of Non-Diagonal Two-Body Matrix Elements on the Binding Energy of Closed Shell Nuclei // *Phys. Rev. C.* 2012. V. 86. P. 054324.
18. *Modarres M.* Local Density Approximation for Alpha-Particle Binding Energy // *J. Phys. G.* 1984. V. 10. P. 251.
19. *Modarres M., Moshfegh M. H., Mariji H.* Lowest Order Constrained Variational and Local Density Approximation Approach to the Hot Alpha Particle // *Can. J. Phys.* 2002. V. 80. P. 1.
20. *Coraggio L. et al.* Ground-State Properties of Closed-Shell Nuclei with Low-Momentum Realistic Interactions // *Phys. Rev. C.* 2003. V. 68. P. 034320.
21. *Coraggio L. et al.* Nuclear Structure Calculations and Modern Nucleon–Nucleon Potentials // *Phys. Rev. C.* 2005. V. 71. P. 014307.
22. *Coraggio L. et al.* Nuclear Structure Calculations with Low-Momentum Potentials in a Model Space Truncation Approach // *Phys. Rev. C.* 2006. V. 73. P. 014304.

Received on July 22, 2013.